ISSN 1063-780X, Plasma Physics Reports, 2022, Vol. 48, No. 6, pp. 693–710. © Pleiades Publishing, Ltd., 2022.
Russian Text © The Author(s), 2022, published in Uspekhi Prikladnoi Fiziki, 2022, Vol. 10, No. 2, pp. 109–131.

APPLIED PHYSICS

Decomposition of CO_2 in Atmospheric Pressure Barrier Discharge (Analytical Review)

Yu. A. Lebedev[a] and V. A. Shakhatov[a, *]

[a] *A. V Topchiev Institute of Petrochemical Synthesis, Russian Academy of Sciences, Moscow, 119991 Russia*

**e-mail: lebedev@ips.ac.ru*

Received March 10, 2022; revised March 10, 2022; accepted March 10, 2022

Abstract—An analytical review of the results of studies of the decomposition of carbon dioxide in a barrier discharge at atmospheric pressure is presented. The decomposition of carbon dioxide CO_2 in a barrier discharge occurs under nonequilibrium conditions as a result of dissociative excitation of the molecule by electron impact. It has been established that the degree of decomposition of carbon dioxide α and the energy efficiency of the device η do not exceed $\alpha \le 70\%$ and $\eta \le 23\%$, respectively. These parameters depend on the geometry of the discharge, on the power deposited in the discharge, on the gas flow rate, and on the gap between the electrodes. One of the promising ways to increase the barrier discharge efficiency is to fill the gap between the electrodes with granules of various materials, including catalysts.

Keywords: barrier discharge, carbon dioxide, decomposition, plasma catalysis

DOI: 10.1134/S1063780X22700209

INTRODUCTION

The growing needs of modern society for energy have significantly increased the consumption of carbonaceous fossil fuels (coal, natural gas and oil) on an unprecedented scale [1]. CO_2 emissions from fuel combustion in power engineering and transport have a negative impact on human life. In addition to adverse environmental impacts, CO_2 emissions are a waste of a natural source of carbon.

Actual problems solved by many researchers are the problem of reducing CO_2 emissions in technological processes, as well as the problem of decomposition and utilization of the resulting carbon dioxide.

Utilization of CO_2 is associated with the development of a highly efficient and cost-effective technology for the decomposition of pure CO_2 and in its mixtures with molecular and inert gases. This makes it possible to use CO_2 as a feedstock for the industrial production of synthetic fuels (synthetic gas $CO + H_2$, methane CH_4, etc.) and chemical products (methanol CH_3OH, formic acid HCOOH, etc.) [2–8].

CO_2 decomposition can be carried out by various methods [9–13]. Among them, a special place is occupied by the method of plasma-chemical decomposition of CO_2 using a weakly ionized low-temperature plasma of gas discharges and hybrid methods with simultaneous usage of plasma and catalytic materials. A feature of the plasma-chemical method is the low energy consumption for the decomposition of CO_2, the compactness of gas-discharge devices and their low material consumption. The decomposition of CO_2 in various gas discharges has not been fully studied and is being intensively studied. Increased attention is paid to the use of an atmospheric pressure barrier discharge (BD) for the decomposition of CO_2 in a subsonic gas flow.

The work presents an analytical review of the current state of research on CO_2 decomposition in an atmospheric pressure barrier discharge. The review does not claim to be complete and is aimed at showing the main trends observed when using a barrier discharge to decompose CO_2.

PARAMETERS AND DESIGN OF DISCHARGE DEVICES BASED ON A BARRIER DISCHARGE FOR CO_2 DECOMPOSITION

Results of studying CO_2 decomposition in atmospheric pressure BD in a subsonic gas flow are given in reviews [9–13] and in numerous original papers [14–59].

When comparing CO_2 utilization devices, a number of criteria are used. In particular, these are the degree of CO_2 decomposition $\alpha(\%)$ and the energy efficiency of the CO_2 decomposition device $\eta(\%)$.

The degree of CO_2 decomposition $\alpha(\%)$ is calculated by the formula:

$$\alpha(\%) = \frac{G^{CO_2}(\text{inlet}) - G^{CO_2}(\text{outlet})}{G^{CO_2}(\text{inlet})} \times 100\%,$$

where G^{CO_2}(inlet) and G^{CO_2} (outlet) are the mass flow rates of CO_2 ($g \times s^{-1}$) at the inlet and outlet of the reactor.

The energy efficiency of the device for CO_2 decomposition $\eta(\%)$ is determined by the expression

$$\eta(\%) = \alpha(\%)\frac{\Delta H^{o}_{298,eV}(OC{-}O)}{E_m^{eV}}.$$

Here $\Delta H^{o}_{298,eV}(OC{-}O)$ is the OC–O bond breaking energy of the resulting reaction

$$CO + M \rightarrow CO + (1/2)O_2 + M,$$

and it is 2.9 eV/mol at 298.15 K. E_m^{eV} denotes the specific energy (in eV) per CO_2 molecule entering the reactor.

In studies of CO_2 decomposition in BD, the devices are widely used, in which plasma is formed in the gap between a pair of coaxial dielectric tubes with conductive plates on the outer surface of the outer tube and the inner surface of the inner tube, as well as between the coaxial outer quartz tube with a conductive lining on the outer surface and an inner metal rod.

Table lists the data on the characteristics of devices with BD [14, 48, 51, 55, 59], in which systematic studies of CO_2 decomposition were carried out.

The parameters given in Table served as initial data in the theoretical BD models developed in [24, 27, 29, 30, 41–44, 49, 50, 59] for studying the mechanisms of CO_2 decomposition.

NUMERICAL SIMULATION AND THE MECHANISM OF CO_2 DECOMPOSITION IN A BARRIER DISCHARGE

In BD plasma in CO_2 and CO_2-containing mixtures, the characteristic values of the reduced electric field E/N are in the range from 100 to 200 Td. In this range of the E/N variation, plasma is dominated by plasma-chemical reactions involving high-energy electrons [9–12, 60–63]. According to the calculation results, the average energy $\langle\varepsilon\rangle$ and electron density n_e varies in the range from 1 to 10 eV [61–63] and is $\approx 10^{10}$–10^{14} cm^{-3}, respectively. The rate constants of plasma-chemical reactions mainly depend on the E/N value (or $\langle\varepsilon\rangle$) and the cross sections of processes and reactions.

It was shown in [24] that the decay of a CO_2 molecule in a BD through the vibrational continuum of the molecule is of secondary importance. The energy consumption of electrons is mainly due to the excitation of electronic states and single ionization of the CO_2 molecule by electron impact. The production of molecular ions is limited by the recombination reaction with the formation of neutral CO_2 molecules.

In [29], a non-stationary zero-dimensional collisional-radiative BD model is presented (W_V = 10.6 W cm^{-3}, T_g = 300 K, f_T = 35 kHz, $n_e = 5 \times 10^{13}$ cm^{-3}, $\tau_L = 0.52$–5.15 s, E/N ≥ 100 Td) [20, 24] to study the mechanism of CO_2 decomposition, as well as to determine its operational characteristics α and η. Particular attention was paid to the description of vibrational kinetics and plasma-chemical reactions involving excited CO_2 molecules at vibrational levels up to the limit of dissociation of the CO_2 molecule (up to 5.5 eV). The electron energy distribution function (EEDF) was determined as a function of E/N using processes, reactions, and collision cross sections of electrons with CO_2, taken from Refs. [64, 65]. For processes of vibrational excitation of CO_2 molecules by electron impact, we considered multiquantum transitions $00^0v_3 \rightarrow 00^0w_3$ between vibrational states (00^0v_3) and (00^0w_3) of the asymmetric mode of the CO_2 molecule. The rate constants of processes and reactions were calculated depending on $\langle\varepsilon\rangle$ using the found EEDF. The solution of the equations for the concentrations of plasma particles was found as a function of the residence time of the gas τ_L in the discharge volume.

As a result of the calculations, it was found that the average electron energy $\langle\varepsilon\rangle$ in the BD varies in the range from 1.4 to 2.2 eV. The calculated vibrational temperature T_3 corresponding to the asymmetric vibrational mode of the CO_2 molecule is 950 K. In BD, the decomposition of the CO_2 molecule occurs as a result of direct electron impact. The contribution of reactions involving CO_2 and vibrationally excited $CO_2(00^0v_3)$ molecules to the CO_2 decomposition rate is insignificant, which confirms the results of [24].

It was shown in [29] that when vibrational kinetics is included in the model, the calculations do not reproduce the decrease in the energy efficiency of the device η with the specific energy E_m^{eV} observed in the experiment [15, 20, 22, 23, 26, 30–33, 38–40, 47, 48], which is especially expressed in the range of $E_m^{eV} \geq$ 4 eV/mol. The calculated α value increases from 6 to 25% with an increase in E_m^{eV} from 3.5 to 14 eV/mol, and the η value changes from 4.7 to 5%.

In a later work [30], a simplified kinetic model of CO_2 decomposition was elaborated, including 17 reactions involving 9 chemical compounds. It has been shown that this model reproduces the main mechanisms of CO_2 decomposition in BD established in earlier works [24, 27, 29].

The work [41] is a continuation of [30]. It proposes a one-dimensional model that describes the decomposition of CO_2 in BD in the hydrodynamic approximation. The model uses a simplified kinetic scheme of reactions from [30].

In [43, 44, 50], a comparative analysis of data on the cross sections and rate constants of processes and reactions used in various plasma-chemical models of BD was performed. A detailed analysis and generalization of the results of calculations of the energy spectrum of electrons using different models was performed in [66, 67].

In a recent paper [59], a kinetic model was proposed for the interpretation of the results of determining α and η, on the basis of which the decomposition mechanism of CO_2 in BD was considered in detail ($W = 150$ W, $f_T = 25$ kHz, $G_g = 0.42–1.7$ cm^3/s, $\tau_T = 4.2–2.1$ s, $E_m^{eV} = 12.8–29.55$ eV/mol, $T_g = 373$ K) in a mixture $(100\%\text{-X})CO_2 + XO_2$ ($0\% \le X \le 50\%$) when spherical barium titanate $BaTiO_3$ granules are placed in the reactor. The model is based on the results obtained earlier in [10, 24, 27, 30, 36, 41–44, 49, 50, 54, 57, 68]. The model takes into account that the addition of granules to the discharge gap lowers the breakdown voltage and increases E/N and $\langle\varepsilon\rangle$ in the BD [10, 36, 68]. The initial parameters in the model are the data obtained in [54, 57]. They found that $\langle\varepsilon\rangle$ is 5.9 eV at E/N = 200 Td in a reactor with a packed layer of granules. The average electron energy $\langle\varepsilon\rangle$ increases with the increase in E_m^{eV}.

In [59], the dependences of the EEDF, the $\langle\varepsilon\rangle$ values and the concentration of molecular oxygen $[O_2]$ on E/N were studied using the program developed in [69] for determining the EEDF and its main aspects. The EEDF calculations confirm the conclusion [54], based on the results of studying the emission spectra of electronically excited emitting states of CO_2^+ ions, that the fraction of high-energy electrons ($\varepsilon \ge 13.8$ eV) at $E_m^{eV} = 8.4$ eV/mol in EEDF is not large. In [59], it was found that the average electron energy $\langle\varepsilon\rangle$ increases with increasing E/N. The addition of molecular oxygen O_2 to CO_2 leads to an increase in η. An increase in the content of molecular oxygen X to 50% in a mixture of $(100\%\text{-X})CO_2 + XO_2$ at E/N = 100 Td leads to an increase in η from 3.7 to 4 eV. As a result, the fraction of high-energy electrons in the EEDF increases and, thus, the degree of CO_2 decomposition, the concentration of O_2 molecules in electronically excited states, the concentrations of O atoms in the ground (^{3}P) and in the metastable (^{1}D) states, the rates of chemical reactions that are inverse to the reactions of CO_2 decomposition increase.

Thus, the results obtained in [24, 27, 29, 41, 42, 49, 59] indicate that in the atmospheric pressure BD, CO_2 decomposition occurs from the ground state as a result of electron impact, mainly through the excitation of electronic states of the molecule with its subsequent disintegration (dissociative excitation of CO_2 molecules). The construction of a model of CO_2 decomposition in a multicomponent plasma that reliably predicts the operational characteristics of a BD-based discharge device is far from being complete. This produces additional difficulties in determining the operational characteristics of the device depending on the controlled BD parameters.

DEGREE OF DECOMPOSITION (α) AND ENERGY EFFICIENCY (η) OF BARRIER-DISCHARGE-BASED DISCHARGE DEVICES DURING CO_2 DECOMPOSITION (EXPERIMENTAL RESULTS)

In [14], the measured degree of CO_2 decomposition in BD at $T_e = 1–3$ eV, $T_g = 415–515$ K, W = 100 W, and p = 500 Torr is $\alpha \approx 30\%$. At gas recirculation in the reactor, this α value was reached within 20 min, counted from the time of the BD initiation. It is shown that in a flow reactor with a gas volume flow rate G_g of up to 22 cm^3/s, at an increase in specific energy E_V^J from 18 to 800 J/cm^3 ($E_m^{eV} = 4.2–185.8$ eV/mol), the degree of CO_2 decomposition α increases from 3to 30% while reducing the energy efficiency of the device η from 1 to 0.4%. Later works [15–59] are devoted to the search for adjustable BD parameters (f_T, V_A, V_b, V_d, G_g, L, d_g, E_m^{eV}, W_A, T_g, T_W, $d\eta$, η_d, d_g—for definitions, see the footnote to Table), at which α and η take maximum values. The performance of the device was improved by improving the design of the discharge device (material and geometry of the electrodes and reactor, power source, etc.) and adding argon Ar, helium He and molecular nitrogen N_2 and oxygen O_2 to the initial CO_2.

DEPENDENCE OF α AND η ON GAS TEMPERATURE TG AND TEMPERATURE OF REACTOR WALLS T_W

The rate constants of chemical reactions in the gas phase and on the reactor surface depend on the translational gas temperature T_g and the reactor surface temperature T_W, respectively. The results of [15, 20, 56] indicate that this dependence should be taken into account when developing a BD-based device.

It was shown in [15] that when the BD reactor was cooled, the α value increased by 0.5–3%. The reactor was cooled by increasing the volumetric gas flow.

In a later work [20], it was shown that preheating of CO_2 entering the reactor has an insignificant effect on its degree of decomposition α. As the temperature T_W of the reactor wall increases from 303 to 443 K, the

degree of CO_2 decomposition increased linearly from 26 to 28.5%.

The dependence of the degree of CO_2 decomposition on temperature T_W found in [20] differs from the results of [15, 26]. It was found in [26] that the rate of the CO and O recombination reaction increases with increasing reactor wall temperature T_W. The CO content at the reactor outlet decreases with increasing temperature T_W, which agrees with the results (the degree of CO_2 decomposition decreases) [15].

Taking into account the results of [15, 26], a discharge device with a cooled reactor was developed in [56]. It was established in [56] that cooling the reactor to room temperature increases the degree of CO_2 decomposition by 10%. The use of reactor cooling increases η by 6 times compared to similar device without cooling. The improvement in device performance in [56] is explained by a decrease in the rate of heterogeneous recombination of CO and O due to a decrease in the temperature of the reactor surface.

Thus, in order to provide the best performance parameters of the discharge device, the temperature of the reactor wall should be kept as low as possible [11, 47].

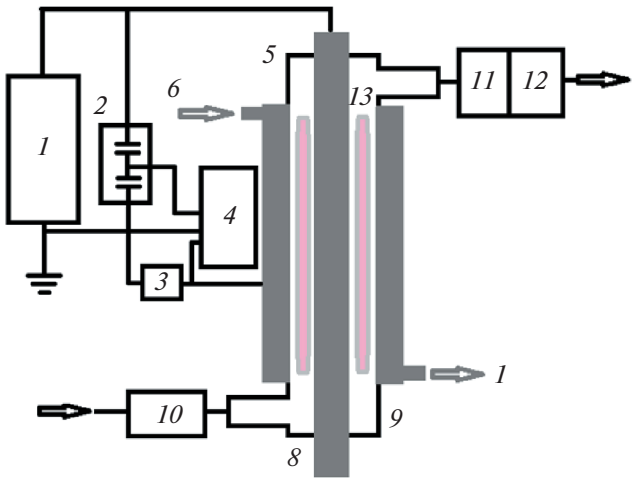

Fig. 1. *1*—barrier discharge power supply; *2*—measuring capacities; *3*—measuring resistance; *4*—oscilloscope; *5*—reactor; *6* and *7*—inlet and outlet of conductive NaCl solution, respectively (or outer ground electrode); *8*—inner (high-voltage) electrode; *9*—discharge tube; *10* and *11*—gas-vacuum system for supplying and pumping gas, respectively; *12*—gas chromatograph; *13*—discharge volume.

DEPENDENCE OF THE DEGREE OF CO_2 DECOMPOSITION AND THE ENERGY EFFICIENCY OF THE DEVICE ON THE ADJUSTABLE BD PARAMETERS (f_T, W_A, G_g, L, d_g, $d\eta$, V_A, V_b, V_d AND E_m^{eV})

Of the vast majority of studies of the dependence of the operational characteristics of the discharge device on the controlled BD parameters, we focus on the discussion of the results of works [51, 55], in which systematic studies of the dependences of α and η on the BD parameters were performed.

The results of measurements of the dependences of α and η on the power W_A absorbed by the BD plasma and on the frequency f_T of the high-voltage voltage applied to the inner electrode of the reactor are presents in [55]. The plasma-chemical reactor (Fig. 1) was a quartz tube with inner and outer diameters of 16 and 20 mm, respectively. It had a cooling jacket along the entire length. The tube was cooled with a saturated NaCl solution, which served as a ground electrode. A cylindrical steel electrode with a diameter of 12 mm and length of 280 mm was placed coaxially inside the quartz tube. A high voltage with a frequency f_T from 10 to 30 kHz was applied to the inner electrode. The maximum voltage amplitude V_A was 15 kV. The size of the discharge gap d_g and tube thickness d_ε coincided and was 2 mm. The volume flow rate of CO_2 at the inlet to the reactor was $G_g = 3.3$ cm^3/s. The component composition of the gas at the outlet of the reactor was determined in real time using a gas chromatograph. CO_2, CO, and O_2 were present in the outlet gas. The concentrations of CO and oxygen atoms O were in a 1:1 stoichiometric ratio. No carbon formation was observed. It was shown in [55] that at a constant volumetric flow rate of carbon dioxide $G_g = 3.3$ cm^3/s, as the discharge voltage increases from 5700 to 7300 V, the power W_A absorbed by the plasma increases from 56 to 143 W (E_m^{eV} = 3.9–100 eV/mol). The degree of CO_2 decomposition increases from ≈5 to ≈13% (at f_T = 13.5 kHz). The η value does not change and is 3.7%. The dependence of η on E_m^{eV} agrees with that calculated in [29]. It differs from the corresponding dependence established in [11] from the processing of experimental data [15, 20, 22, 23, 26, 30–33, 38–40, 47, 48]. The maximum values of α_M and η_M are ≈13 and ≈3.7%, respectively, at f_T = 13.5 kHz and E_m^{eV} = 100 eV/mol. The dependences of operational characteristics on the frequency of high voltage, obtained in [55] are consistent with the corresponding dependences presented in [30, 46].

In [18, 30, 46, 55], a weak dependence of the degree of CO_2 decomposition and energy efficiency of the device on the applied voltage frequency f_T in the range of 10–50 kHz at a constant active BD power W_A, despite the fact that at increasing frequency, the number of filamentous formations filling the discharge volume increases. It was found in [46] that with an increase in the frequency f_T from 6.2 to 28.6 kHz, the of α and η values decrease from 22 to 17.5% and from 15.3 to 12.5%, respectively, at W_A = 55 W (E_m^{eV} =

3.9 eV/mol) and $G_g = 3.3$ cm^3/s. It was found in [55] that with an increase in the frequency f_T from 10 to 20 kHz, the α and η values decrease from ≈8.2 to ≈7.2% and from ≈3.7% to ≈3.3% (at constant W_A = 91 W and $G_g = 3.3$ cm^3/s), respectively. The dependence of the parameters α and η observed in the experiment can be explained by the fact that with an increase in f_T from 10 to 20 kHz, the voltages V_b, V_d and V_A are reduced from 4800 to 4400 V, from 3974 to 3643 V and from 7000 to 5600 V, respectively. As a result, the charge Q_{tc} values due to the conduction current and the electric field strength V_d/d in the discharge gap decrease. The fraction of high-energy electrons in the EEDF that cause the decomposition of CO_2 in the reaction of dissociative excitation of the CO_2 molecule decreases. Thus, the important BD parameters are the maximum value of the voltage across the discharge gap V_d and the minimum value of the voltage V_b applied to the high-voltage electrode, above which an electrical breakdown occurs in the discharge gap. The V_d value determines the electric field strength V_d/d in the BD. The V_b value determines the active power W_A supplied to the reactor and the charge Q_{tc} due to the conduction current. The degree of CO_2 decomposition is directly proportional to the active power W_A (or the charge Q_{tc} due to the conduction current) [55]. This indicates that the mechanism of carbon dioxide decomposition in BD is due to the reaction of dissociative excitation of a carbon dioxide molecule by electron impact [10, 24, 27, 29, 30, 41, 42, 49, 55]. The maximum value of the energy efficiency of a discharge device based on BD is low [20, 22, 31, 36, 55].

In [51], the number of adjustable parameters, according to which the optimization of the operational characteristics of a BD-based discharge device, was noticeably increased compared to their number from [55]. It studied the dependence of the degree of decomposition of CO_2 and the energy efficiency of the device: on the frequency f_T of the applied voltage; volumetric gas flow G_g; on the specific energy E_m^{eV} supplied from the power source to the reactor; on the discharge length L, discharge gap d_g and tube thickness $d_ε$ of the reactor. Regression models were elaborated to determine the relative importance of the BD parameters in estimating α and η. Various designs of the inner and outer electrodes are proposed to improve the operational parameters of the discharge device. The atmospheric pressure reactor consisted of a quartz tube (with an outer diameter 25 mm and a variable inner diameter of 20–22 mm), inside which the electrode is axially located (with an outer variable diameter of 15–17 mm). The discharge gap d_g and the thickness of the reactor tube dη varied in the ranges from 2.5 to 3.5 mm and from 1.5 to 2.5 mm, respectively. The conductive lining (outer electrode) was attached to outer surface of the quartz tube. In the experiment, the length of the outer electrode varied from 60 to 140 mm. The outer electrode served as the ground electrode. To study the effect of the design of the outer and inner electrodes on CO_2 decomposition, the following details were used in the experiment: rod and screw inner electrodes made of stainless steel; mesh stainless steel and aluminum foil outer electrodes. The voltage V_A (up to 30 kV, frequency f_T from 8 to 11 kHz) was applied from a high voltage source to the inner electrode. The applied voltage V_A and the total discharge current I were measured. The power W_A absorbed by the BD plasma was determined from the area of the parallelogram in the volt–coulomb characteristic [36, 70]. Pure CO_2 was used as a source gas (flow rate $G_g \sim 0.42$–2.2 cm^3/s). The composition of the gas at the outlet of the BD was measured in real time using a gas chromatograph. Dependences of the performance characteristics on the frequency of the high-voltage voltage obtained in [51] are consistent with the corresponding dependences presented in [30, 46, 47, 55, 71]. In [47, 51], a weak dependence of the degree of CO_2 decomposition and energy efficiency of the device on the frequency of the applied voltage in the range of 8–30 kHz at a constant active power W_A of the barrier discharge was found. It was also found in [47] that the degree of decomposition of CO_2 and the energy efficiency of the discharge device changes slightly as the frequency increases from 15 to 30 kHz. In [51], it is shown that the α and η values for the BD-based discharge devices (stainless steel rod inner and mesh outer electrodes, $E_m^{eV} = 22.3$ eV/mol, W_A = 40 W, $G_g = 0.42$ cm^3/s, $L = 100$ mm, $d_g = 2.5$ mm and $d_ε = 1.5$ mm) decrease slightly at the frequency f_T increasing in the range from 8 to 11 kHz. The α and η values are in the ranges from 26 to 24% and from 2.9 and 2.8%, respectively. The dependences of α and η on the BD frequency observed in [30, 46, 47, 51, 55, 71] are explained by a decrease in: the maximum voltage value on the electrodes VA, the minimum the value of the voltage V_b, above which an electrical breakdown occurs in the discharge gap and the maximum voltage V_d value across the discharge gap during the barrier discharge. In the experiment [51], the dependence of the operational characteristics of the device on the specific energy E_m^{eV} in the range from 24 kJ/L (5.6 eV/mol) to 120 kJ/L (27.9 eV/mol) was studied by two ways by: (1) increasing the active power W_A supplied to the reactor from 10 to 50 W at a constant volume flow rate $G_g = 0.42$ cm^3/s; (2) when the gas volume flow G_g decreases from 2.1 to 0.42 cm^3/s at a fixed value of the active power W_A = 50 W. The experiments were performed at a constant frequency f_T = 9 kHz. The dependence of α on the specific energy E_m^{eV} obtained in [51], confirms the results of numerous works [14–50, 52–59]. The dependence of

η on E_m^{eV} found in [51] differs from that presented in [55] and coincides with the results of [14–50, 52–54, 56–59]. It was established in [51] that η noticeably decreases from 9 to 2.3% with an increase in E_m^{eV} from 5.6 eV/mol (W_A = 10 W) to 27.9 eV/mol (W_A = 50 W) in BD (at G_g = 0.42 cm^3/s, L = 100 mm, d_g = 2.5 mm and dη = 1.5 mm). The degree of decomposition of carbon dioxide α with increasing specific energy E_m^{eV} increases from 17.4 to 22.4%. With an increase in the specific energy, an increase in the number and amplitude of conduction current pulses was observed, which leads to an increase in the degree of CO_2 decomposition. With a decrease in the gas volume flow G_g from 2.1 to 0.42 cm^3/s and with an increase in the specific energy E_m^{eV} from 5.6 to 27.9 eV/mol in BD (at W_A = 50 W, L = 100 mm, d_g = 2.5 mm and d_ε = 1.5 mm) the degree of decomposition of carbon dioxide α increases from 12.6 to 22.4%, while the energy efficiency η drops from 6.6 to 2.3%. The maximum α_M value ≈22.4% is observed at the minimum volumetric gas flow rate G_g = 0.42 cm^3/s. At fixed BD parameters, an increase in G_g reduces the residence time of gas particles in the discharge region. As a result, the degree of CO_2 decomposition decreases, and the energy efficiency of the discharge device η increases.

Thus, the nature of the change in α and η and their values depend on the method of changing the specific energy E_m^{eV} (when the voltage on the electrodes changes and the flow rate is constant, or when the gas flow rate changes and the voltage is constant). Regulation of the specific energy by changing the volumetric gas flow has a greater effect on α and η than changing the active power supplied to the reactor.

The results of [51] confirm the data obtained earlier in [22, 30] that η and α depend on the longitudinal and transverse dimensions of the discharge volume at the same specific energy. It was found in [30] that for a certain size of the discharge gap (of ≈3.3 mm), the minimum number of streamers is formed in it. As a result, the effective discharge volume, in which CO_2 decomposes, decreases. The η and α values decrease. It was found in [51] that (at f_T = 9 kHz, E_m^{eV} = 5.6–27.9 eV/mol, G_g = 0.42 cm^3/s, L = 100 mm and d_ε = 1.5 mm), an increase in the size of the discharge gap d_g from 2.5 to 3.5 mm reduces both the energy efficiency of the discharge device (rod inner and mesh outer stainless steel electrodes) and the degree of CO_2 decomposition. At 5.6 eV/mol and an increase in d_g from 2.5 to 3.5 mm, the α and η values decrease from 17.3 to 13.7% and from 9.2 to 7.2%, respectively. At a higher specific energy of 27.9 eV/mol, such an increase in d_g led to a decrease in α from 22.1 to 16.8%, and η from 2.4 to 1.8%. An increase in the discharge gap leads to [72]: an increase in the residence time of gas in the discharge volume; a decrease in the specific energy absorbed by the plasma per unit volume; a slight decrease in the amount of charge due to the bias current and conduction current in BD. In [72], it is assumed that a "partial discharge" occurs in a larger gap. Streamers cannot ensure the formation of a microdischarge that shunts the discharge gap. This leads to a decrease in α and η. The formation of the "partial discharge" plays a more noticeable negative role in CO_2 decomposition than a positive role associated with an increase in the residence time of the gas in the discharge volume. It was shown in [51] that (at f_T = 9 kHz, E_m^{eV} = 24–120 kJ/L (5.6–27.9 eV/mol), G_g = 0.42 cm^3/s, d_g = 2.5 mm and d_ε = 1.5 mm), an increase in the longitudinal dimension of the discharge volume L increases both η and α. At 5.6 eV/mol and an increase in L from 60 to 140 mm, the α and η values increase from 15.6 to 18.8% and from 8.2 to 9.8%, respectively. At a higher specific energy value of 27.9 eV/mol, an increase in L leads to an increase in α from 19 to 25.2%, and η from 2.2 to 3%. The observed dependences of α and η on the length of the discharge volume L are explained by the competition of the following phenomena [51, 73]: (1) an increase in the discharge volume due to the length of the inner metal electrode L leads to an increase in the residence time of the reagents τ_L in the discharge volume; (2) cooling of the discharge volume as a result of thermal conduction; (3) decrease in specific energy E_m^{eV} (at a constant power W_A supplied to the reactor).

The results of [17, 18, 23, 39, 47, 51] indicate that the operational characteristics of the discharge device depend on the material and thickness of the dielectric electrode insulation dη.

In [17, 18, 23], new dielectric materials $Ca_{0.8}Sr_{0.2}TiO_3$ with the addition of material 0.5 wt % $Li_2Si_2O_5$ and glass 0.5–5 wt % $CaOB_2O_3$–SiO_2 were fabricated. The materials are recommended for application as dielectric insulation of electrodes. It was shown in [17, 18] that the use of $Ca_{0.8}Sr_{0.2}TiO3$ with the addition of 0.5 wt % $Li_2Si_2O_5$ as the dielectric insulation of electrodes increases α by a factor of 9 compared to that obtained when silica glass is used. In a later work [23], it was found that the use of the $Ca_{0.8}Sr_{0.2}TiO_3$ material with glass additives of 5 wt % $CaO–B_2O_3–SiO_2$ leads to an increase in α by 2.6 times, and η increases by 3 times compared to what is obtained when using $Ca_{0.8}Sr_{0.2}TiO_3$ with glass additives of 0.5 wt % $CaO–B_2O_3–SiO_2$. The improvement in the operational characteristics of the device is associated with the formation of a filamentary type of BD, characterized by high conduction current pulses at a lower output voltage of the BD power supply.

Thus, the results of [17, 18, 23] show that dielectric materials $Ca_{0.8}Sr_{0.2}TiO_3$ with the addition of 0.5 wt %

$Li_2Si_2O_5$ and glass additives of 0.5–5 wt % CaO–B_2O_3–SiO_2 make it possible to increase the α and η values at lower voltages on the high-voltage electrode.

It was established in [30] that the physicochemical properties of BD weakly depend on whether quartz (SiO_2) or aluminum oxide (Al_2O_3) is used as the dielectric insulation of electrodes in a wide range of BD parameters. It is noted that the barrier discharge is more stable when Al_2O_3 electrodes are used as dielectric insulation. In [39], when studying the deposition of a conductive layer on a dielectric coating, it was noted that the conductivity of the dielectric coating is an important parameter affecting the physicochemical properties of BD. The results of [39] confirm the conclusions of [17, 18, 23]. The results [47] indicate that an increase in the thickness of the dielectric insulation of the electrodes leads to higher α and η values. This is true when using aluminum oxide Al_2O_3 or quartz SiO_2 as dielectric insulation of electrodes instead of mullite (compounds of Al_2O_3 with SiO_2) and pyrex (hardened borosilicate glass made from 80% pure sand, 4% soda, 2.5% alumina and 13% boron). The data obtained in [51] do not confirm the results of [47]. It found there that (at f_T = 9 kHz, E_m^{eV} = 5.6–27.9 eV/mol, G_g = 0.42 cm^3/s, d_g = 2.5 mm, and L = 100 mm) with an increase in the thickness of the quartz tube dη the degree of decomposition of carbon dioxide α and the energy efficiency of the discharge device (rod inner and mesh outer electrodes made of stainless steel) η decrease at a fixed value of the specific energy E_m^{eV}. At E_m^{eV} = 5.6 eV/mol and an increase in d_ε from 1.5 to 2.5 mm, the α and η values decrease from 17.2 to 14% and from 9.2 to 7.2%, respectively. At a higher specific energy E_m^{eV} = 27.9 eV/mol, an increase in d_ε leads to a decrease in α from 22.4 to 18.8%, and η from 2.8 to 2%. The dependences of the α and η values on d_ε, observed in [51], are explained on the basis of the results of [72] by a decrease in the residence time of the gas in the discharge volume τ_L and the amount of charge due to the bias current and conduction current of BD. In the experiment [51], the discharge gap was kept constant. The decrease in the residence time of the gas in the discharge volume is due to the fact that the discharge volume decreased by 10.3% due to the simultaneous decrease in the inner diameter of the outer quartz tube and the outer diameter of the inner electrode.

Thus, the α and η values for BD depend on the outer parameters of the discharge: frequency of the applied high voltage f_T; power W_A supplied to the reactor; volumetric gas flow G_g; longitudinal size of the discharge volume L; discharge gap d_g; thickness of the dielectric barrier d_ε. To increase α and η, it is necessary to maintain high values of the residence time of the gas in the discharge volume and the charge due to the bias current and conduction current of the BD. In [51], empirical relationships are proposed to describe the dependence of α and η on the controlled BD parameters, which are obtained from processing experimental data η using regression models:

$$\alpha = 34.3401|f_T|^{-0.0448}|W_A|^{0.1634}|G_r|^{-0.3839} \times |L|^{0.2527}|d_g|^{-0.6999}|d_\varepsilon|^{-0.3593},$$

$$\eta = 6.4876|f_T|^{-0.0415}|W_A|^{-0.8367}|G_r|^{0.6158} \times |L|^{0.531}|d_g|^{-0.7004}|d_\varepsilon|^{-0.3605}.$$

Here, numerical coefficients and exponents are obtained as a result of multiparameter fitting of the product of functions $|f_T|^{a_i}$, $|W_A|^{b_i}$, $|G_g|^{c_i}$, $|L|^{d_i}$, $|d_g|^{e_i}$ and $|d_\varepsilon|^{f_i}$ by the least squares method for the α and η values measured in the experiment. Empirical relationships are valid in the following ranges of adjustable parameters: f_T = 8–11 kHz, W_A = 10–50 W, G_g = 25–125 mL/min (0.42–2.1 cm^3/s), L = 60–140 mm, d_g = 2.5–3.5 mm and d_ε = 1.5–2.5 mm. The experimental results coincide with the predicted data α and η with a maximum relative error of ≈6%. Empirical ratios determine the relative significance of the adjustable parameters of the discharge device in the evaluation of α and η, which are located in the order of decreasing significance:

$$G_g \approx W_A > d_g > L > d_\varepsilon > f_T.$$

INCREASING α AND η THROUGH REACTOR DESIGN IMPROVEMENTS

In [15, 21, 34, 47, 51], efforts were made to improve the operational characteristics of the discharge device by improving the design of the reactor. In [15], the dependence of the degree of CO_2 decomposition in BD on the high-voltage electrode material (Cu, Au, Rh, Fe, Pt, and Pd) was studied. When using high-voltage electrodes made of Cu and Au, α increases by 1.5 times compared to what is obtained when using an electrode made of Fe. The energy efficiency of the discharge device increases in 3 times when using high-voltage electrode made of Au compared to what is obtained when using an electrode made of Rh under the same conditions. We note that the materials differ in cost and susceptibility to chemical corrosion and ion-plasma sputtering. The relative importance of the effect of the material on the operational characteristics of the discharge device is reflected by the following hierarchy [15]:

$$Cu > Au > Rh > Fe \approx Pt \approx Pd.$$

In [21, 34, 47], a microplasma reactor of a surface BD was developed and improved, in which a solid oxide electrolytic element and a switching power supply are used in the regenerative mode to decompose CO_2. The use in [34] of a microplasma reactor of a sur-

face BD made it possible to decompose CO_2 in an electric field larger than in a conventional BD, as well as to obtain higher concentrations of chemically active compounds compared to the corresponding concentrations formed in a conventional BD. The combination of a solid oxide cell and a pulse power supply eliminates the flow of reverse chemical reactions leading to the formation of O_2. The degree of CO_2 decomposition increases by a factor of 4 compared to that observed in a conventional BD [21]. It was found in [51] that (at $f_T = 9$ kHz, $E_m^{eV} = 5.6–27.9$ eV/mol, $G_g = 0.42$ cm^3/s, $d_g = 2.5$ mm, $d_\varepsilon = 1$, 5 mm and $L = 100$ mm) α and η increase when replacing the stainless steel inner rod and mesh outer electrodes with the corresponding stainless steel helical electrode and aluminum foil electrode. At a fixed low specific energy of 5.6 eV/mol, the values of α and η increase from 17.2 to 20% and from 10 to 10.4%, respectively. At a high specific energy of 27.9 eV/mol such replacement of electrodes leads to an increase in α and η from 22 to 27.2% and from 2.4 to 2.8%, respectively. The improvement in the operational characteristics of the discharge device when replacing electrodes is explained by an increase in the number of microdischarges, the amplitude of current pulses in the power supply circuit of the BD and the charge. The sharp edges of the helical electrode enhance the local electric field near the inner electrode. As a result, intense microdischarges are formed near the edge of the helical electrode, which provide an increase in α and η.

Thus, the research results [18, 20, 22, 30, 32, 34, 36, 39, 45, 74, 75] on the dependences of α and η on specific energy E_m^{eV} and gas volume flow rate G_g indicate an ambiguous choice of its optimal parameters. A compromise is required between energy consumption and the productivity of CO_2 utilization [76]: at a high specific energy E_m^{eV}, the maximum degree of CO_2 decomposition is provided at a low energy efficiency of the discharge device. On the contrary, at a low specific energy E_m^{eV}, the minimum degree of CO_2 decomposition is obtained at a high energy efficiency of the discharge device. A similar problem arises when optimizing a discharge device based on an atmospheric pressure glow discharge [74] and a corona discharge [77].

DEPENDENCE OF α AND η ON THE CONTENT IN THE INITIAL GAS MIXTURE MOLECULAR GASES (NITROGEN N_2, OXYGEN O_2) AND INERT GASES (ARGON Ar, HELIUM He)

It was established in [15, 19, 27, 31] that dilution of CO_2 with inert gases facilitates the initiation of BD due to the formation of Ar and He atoms in metastable states and their involvement in stepwise reactions of ionization by electrons. With an increase in the content of inert gases in a mixture with CO_2, the degree of decomposition of CO_2 in BD increases. Dilution leads to a decrease in the productivity of CO_2 decomposition. Similar phenomena are observed when CO_2 is diluted with Ar in a capacitive RF discharge [78], in a sliding arc [79], and in a nanosecond pulsed corona discharge [80]. CO_2 decomposition in a BD with a compacted layer of barium titanate $BaTiO_3$ granules was studied in [25]. It has been found that low-energy electrons (< 5.5 eV) EEDF, do not participate in the decomposition of CO_2 molecules by electron impact. A significant fraction of the power of the discharge power source supplied to the reactor, as a result of inelastic collisions of low-energy electrons with plasma particles, is spent on excitation of rotational, vibrational degrees of freedom of the CO_2 molecule and inner degrees of freedom of gases (argon Ar, helium He, molecular nitrogen N_2 and oxygen O_2), with which carbon dioxide CO_2 is diluted. The contribution of reactions involving vibrationally excited molecules of CO_2, nitrogen N_2, and oxygen O_2 to the decomposition of CO_2 is limited by VT and VV processes [24]. The increase in the translational temperature of the gas causes a decrease in α in the BD.

It was found in [37] that the α and η values in a mixture of molecular nitrogen N_2 with CO_2 ($50\%CO_2 + 50\%N_2$) coincide with the corresponding values in pure CO_2. This is because the lower CO_2 content in the mixture due to the dilution of CO_2 with molecular nitrogen, is compensated by an increase in the decomposition rate of carbon dioxide due to reactions involving nitrogen molecules in metastable states. It is noted that undesirable by-products of reactions involving N_2 and CO_2 molecules are nitrous oxide N_2O and nitrogen oxides NO_x (nitrogen monoxide NO and nitrogen dioxide NO_2) with concentrations in the range of several 100 ppm (100 NO_x molecules per million particles of plasma gas), leading to environmental pollution. In [54, 57], efforts were made to improve the performance of the discharge device by diluting CO_2 with molecular nitrogen ($20\%CO_2 + 80\%N_2$) or argon ($20\%CO_2 + 80\%$Ar) and adding into the barium titanate $BaTiO_3$ granule reactor. It has been established that the degree of CO_2 decomposition increases with an increase in the content of N_2 or Ar at a constant value of the specific energy $E_m^{eV} = 8.4$ eV/mol. The explanation is that the dilution of CO_2 with molecular nitrogen N_2 ($20\%CO_2 + 80\%N_2$) or argon Ar ($20\%CO_2 + 80\%$Ar) leads to a decrease in the breakdown voltage across the discharge gap and an increase in the electron density and average energy in the BD. Of particular interest are the results of a recent work [59], in which, in order to increase α and η, it was proposed to reduce the rate of the reverse reaction of carbon dioxide decomposition by producing an excess content of molecular oxygen O_2 in the BD plasma in

CO_2 and placing granules of barium titanate $BaTiO_3$ in the reactor. The atmospheric pressure BD reactor ($p = 760$ Torr) consisted of two coaxial quartz tubes located one inside the other. One stainless steel mesh electrode was mounted on the inner surface of the inner quartz tube, and the other was located on the outer surface of the outer quartz tube. The discharge volume of the reactor was filled with spherical granules of barium titanate $BaTiO_3$ (diameter: 3 mm; dielectric constant $\varepsilon \sim 1000$). The filling volume was ≈ 100 cm^3. The void volume of the reactor was ≈ 35 cm^3. The temperature of the reactor wall is $T_W \approx 373$ K. The forward gas temperature at the outlet of the reactor was measured by means of a thermocouple. The forward temperature T_g did not exceed the temperature of the reactor wall. The output power of the barrier discharge power supply was changed to 150 W, the amplitude of the high voltage V_A applied to the electrodes varied up to 20 kV at the frequency $f_T = 25$ kHz. The active power W_A absorbed by the BD plasma was determined by integrating the product of voltage and current. The gas mixture $(100\%\text{-X})CO_2 + XO_2$, $0\% \le X \le 50\%$ was supplied to the reactor. The total volumetric flow rate of the gas mixture G_g varied from 0.42 to 1.7 cm^3/s. The specific energy E_m^{eV} per one molecule of the initial carbon dioxide varied in two ways: with a change in active power W_A (change in voltage V_A at the electrodes) from 46 to 106 W and a constant volume flow rate of the gas mixture $G_g = 0.8$ cm^3/s, as well as with an increase in the volumetric flow rate of the gas mixture from 0.8 to 1.7 cm^3/s ($\tau_T = 4.2$–2.1 s) and a constant value of the active power $W_A = 86$ W. The corresponding values of specific energy E_m^{eV} ranged from 12.8 to 29.5 eV/mol and from 12 to 24 eV/mol. Gas chromatography and absorption spectroscopy in the ultraviolet wavelength range were used to determine the component composition of the decomposition products of a mixture of gases in BR. It has been found that the effect of CO_2 dilution with molecular O_2 on CO_2 decomposition differs from the corresponding effect of N_2, Ar, and He gas additives found in [15, 19, 25, 27, 31, 37, 54, 57]. The degree of CO_2 decomposition depends on the O_2 content in the mixture nonmonotonically. With an increase in the content of O_2 in the mixture up to 5%, the degree of decomposition of carbon dioxide α in BD ($G_g = 0.8$ cm^3/s, $\tau_T = 4.2$ s, $W_A = 86$ W, $p = 760$ Torr, $f_T = 25$ kHz, $E_m^{eV} = 24$ eV/mol) slightly increases from 16 to 17%. With a further increase in the content of O_2 up to 50%, the degree decomposition of carbon dioxide α decreases to 11%. No carbon formation is observed. In [59], the results of studies [24, 26, 54, 57] were confirmed, which indicate that the reaction products of CO_2 decomposition are CO, O_2, and O_3. There is no difference in the α values obtained by adjusting the output power of the power supply or the volume flow of the mixture. An increase in E_m^{eV} from 12 to 29.5 eV/mol leads to a monotonic increase in the degree of decomposition of carbon dioxide α from ≈ 7.5 to 20%. It was established in [59] that the η values decrease with an increase in the percentage of molecular oxygen in a $(100\%\text{-X})CO_2 + XO_2$ mixture. The result obtained in [59] agrees with the results of [31, 37, 54]. It was established in [31, 37, 54] that dilution of CO_2 with molecular nitrogen N_2 or argon Ar reduces η both in a reactor with a packed layer of barium titanate $BaTiO_3$ granules and without granules. In the discharge, active excited states of molecular nitrogen N_2 or argon Ar are formed, which participate in reactions that increase the rate of CO_2 decomposition. It was noted in [59] that oxygen atoms $O(^3P, ^1D)$ and ozone molecules O_3 are also formed in the discharge, reactions involving which, on the one hand, increase the resulting CO_2 recovery rate in the plasma. On the other hand, the reaction of recombination of O atoms and decomposition of ozone O_3, the processes of quenching the metastable state of the oxygen atom ^1D decrease the rates of reverse reactions of CO_2 decomposition. An increase in the percentage of molecular oxygen O_2 to 5% slightly reduced the η value. The η value obtained in [59] is 2% in pure CO_2. It decreases when CO_2 is diluted with molecular oxygen O_2.

PLASMA CATALYSIS/PHOTOCATALYSIS DURING CO_2 DECOMPOSITION IN A BARRIER DISCHARGE

The method of plasma-catalytic decomposition of CO_2 (this term is now widely used) is based on the use of electric discharges and catalytic materials and makes it possible to combine the advantages of catalytic and plasma methods of CO_2 decomposition [10, 68, 81, 82]. It is considered as one of the promising directions for increasing the α and η values [11, 12].

The interaction of the electric field with the granules with which the reactor is filled leads to the fact that, depending on the shape, porosity and permittivity of the granules, the local electric field becomes inhomogeneous and higher than the outer applied field [10]. The local electric field strength near the points of contact between the granules, granules, and surfaces of the outer and inner tubes can be 10–10^4 times higher than in the gap between the granules, depending on the contact angle, curvature, and permittivity of the granules [68, 81]. It has been established that an increase in the permittivity of granules ηg from 1 to 1000 can lead to an increase in the electric field strength in 1.5 times near the points of contact between the granules, granules and surfaces of the outer and inner tubes. A further increase in ηg does not increase the electric field strength [81]. It was shown in [82] that the plasma catalytic decomposition

of substances in solving environmental problems makes it possible to simultaneously increase the energy efficiency of the discharge device and the selectivity of the yield of target reaction products compared to those obtained by decomposition of substances using only BD or when using only catalytic materials. To improve the energy efficiency of the BD-based discharge device η and the selectivity of the target output reaction products in [83–91], the decomposition of CO_2 in mixtures with methane CH_4, water vapor H_2O, and molecular hydrogen H_2 was studied when granules from various materials were introduced into the reactor. The decomposition of pure CO_2 in a BD was studied when the reactor was filled with: silica gel, granules of quartz SiO_2, and calcium titanate $CaTiO_3$ [22, 48]; glass granules [28]; quartz sand, granules of magnesium oxides MgO and calcium CaO [32]; zirconia ZrO_2 granules [33, 48]; barium titanate $BaTiO_3$ granules [28, 36, 40, 48]; quartz wool and Al_2O_3 ceramic granules [32, 48]; glass wool and silica granules SiO_2 [48]; photocatalyst $TiO_2/BaTiO_3$ [45]; catalysts $Ni/\gamma\text{-}Al_2O_3$ [52], Ni/SiO_2 [53], $g\text{-}C_3N_4$ [56], and y/Fe_2O_3 (y = Fe/Ce) [58]. In [32, 92], it was found that the maximum α and η values are obtained when using zirconium dioxide ZrO_2 and oxide calcium CaO. The addition of granules of ZrO_2 and CaO materials to the reactor provides the same energy efficiency of the discharge device as without its presence in the reactor, but makes it possible to increase the degree of decomposition of carbon dioxide α. For example, filling the reactor with ZrO_2 granules makes it possible to double the degree of CO_2 decomposition (α = 38%) compared to the corresponding value without adding granules. The α and η values obtained in [32, 92] are in the range of 30–45% and 5–10%, respectively. In [22, 36, 40, 45], the results of measurements of α and η are given when granules of barium titanate $BaTiO_3$ and calcium $CaTiO_3$ are added to the reactor. It was shown in [22] that the dielectric properties and morphology of spherical calcium $CaTiO_3$ granules (0.42–0.84 mm in diameter) play an important role in CO_2 decomposition. The maximum α_M and η_M values are 20.5% and 4.8%, respectively, at specific energy E_m^{eV} = 12.3 eV/mol. In [45], the decomposition of CO_2 in a BD with a $TiO_2/BaTiO_3$ photocatalyst was described. It is noted that the intensity of UV radiation from the barrier discharge is insignificant compared to the intensity (20–60 mW/cm^2) of an outer ultraviolet radiation source (xenon lamp, λ = 310–380 nm) used to activate photocatalysts. This made it possible to increase performance values up to α = 27– 38.3% and η = 12.2–17% (at E_m^{eV} = 6.5 eV/mol) compared to the corresponding values without using photocatalyst. It has been found that the increase in the α and η values during plasma photocatalysis exceeds the corresponding values obtained only in the photocatalysis of CO_2 decomposition or using only BD. It was found in [40] that the size of barium titanate $BaTiO_3$ granules (180 to 300 μm) and the degree of filling of the discharge volume with them affect the BD parameters and the composition of the reaction products. When small granules (180 μm) are used, the degree of CO_2 decomposition increases to α ≈ 70%. The breakdown voltage of the discharge gap increases. It was established in [36] that the presence of spherical granules of barium titanate $BaTiO_3$ improves the operational characteristics of the discharge device. For granules with a diameter of 1 mm, the α and η values are 30% and 6.3% at E_m^{eV} = 13.9 eV/mol. The addition of barium titanate $BaTiO_3$ granules to the reactor increases the average electric field and the average electron energy compared to the corresponding BD parameters in an empty reactor. This causes an increase in the degree of decomposition of CO_2. In [52], the decomposition of CO_2 in BD into CO_2 was studied when the discharge volume was filled with a $Ni/\gamma\text{-}Al_2O_3$ catalyst. The use of a catalyst leads to higher values of α = 29% and η = 4.5% (at E_m^{eV} = 18.5 eV/mol) than when Al_2O_3 aluminum oxide granules are added to the reactor. The authors explained the increase in α and η by a decrease in the rate of the surface reaction of CO and O recombination in CO_2, due to the action of the catalyst. In [53], the decomposition of CO_2 in BD was studied when a Ni/SiO_2 catalyst was added to the reactor. When using a catalyst, higher degree of decomposition values (α = 23.5% and η = 3.4% at E_m^{eV} = 30.7 eV/mol) are obtained than when granules of barium titanate $BaTiO_3$ or glass are added to the reactor. It is noted in [56] that the use of the $g\text{-}C_3N_4$ catalyst increases the performance characteristics of CO_2 decomposition in BD by a factor of 2 compared to the corresponding values obtained with CO_2 decomposition in BD. The α and η values are 17% and 8.9% at E_m^{eV} = 5.6 eV/mol. In [58], the dependence of the α and η values on the ratio of Fe/Ce mole fractions in a catalyst with a carrier material of iron oxide (Fe_2O_3) activated by cerium Ce is reported. The maximum values of α_M = 24.5% and η_M = 13.6% were obtained using the $y\text{-}Fe_2O_3$ catalyst containing y = 5Fe5Ce. The α_M value is twice the corresponding value achieved when using y = 10Fe (α = 13.3%). The increase in α is explained by the formation of more oxygen vacancies and increased oxygen mobility on the catalyst surface y = 5Fe5Ce.

The results of [48], which present systematic studies of plasma catalysis of CO_2 decomposition in an atmospheric pressure BD, deserve special discussion. The dependences of α and η on the material and diameter of spherical granules d_g added to the reactor, on the dielectric insulator of the electrodes, and the size of the interelectrode gap d_g have been studied in

detail. The material and granules added to the reactor included glass wool, quartz wool, and spherical granules of various materials. The reactor consisted of a tube made of a dielectric material of alumina Al_2O_3 or quartz SiO_2 (Fig. 2). The discharge gap d_g varied depending on the diameter of the inner electrode and was 4.5, 3.5, 2.5, and 2 mm, respectively. The reactor was filled with spherical granules made of quartz SiO_2 (diameter of 1.18–1.4 mm), zirconium dioxide ZrO_2 stabilized with yttria (diameter of 1.4–1.8 mm), alumina Al_2O_3 (diameter of 2.0–2.24 mm), as well as barium titanate $BaTiO_3$ granules. Glass wool or quartz wool was placed at the inlet and outlet of the reactor outside the discharge volume to prevent the movement of granules due to the flow of CO_2 decomposition products. Granule properties (surface acidity, pore volume and size distribution, surface roughness) were studied in detail. Granules were degassed in high vacuum when heated.

The volume flow rate of CO^2 at the inlet to the reactor in the presence of granules in the discharge volume was 0.83 cm^3/s. The g as residence time in the discharge volume was $\tau_T = 5.52$ s. In order to ensure that the residence time of gas particles in the discharge region without granules is the same as the corresponding time at $G_g = 0.83$ cm^3/s, the gas volume flow increased and amounted to 3.3 cm^3/s. The increase in the volumetric flow rate is explained by the fact that the addition of granules to the reactor reduces the residence time of gas particles in the discharge volume τ_T at a constant gas flow rate. The voltage at the outer electrode, the total discharge current, and the active power W_A absorbed by the BD plasma (determined from the area of the parallelogram in the volt–coulomb characteristic) were measured. The temperature of the wall of the reactor tube and the outer electrode was determined from the measurements of the IR intensity and was ≈419 K. The component composition of the gas at the outlet of the reactor was analyzed using a gas chromatograph. CO_2, CO, O_2 were recorded at the discharge output. Carbon deposition on the inner electrode, surfaces of the reactor tube and spherical granules was not detected. It was established in [48] that for three different sizes of spherical granules (with diameters of 1.25–1.4, 1.6–1.8, and 2.0–2.24 mm) made of barium titanate $BaTiO_3$, the obtained $\alpha = 13.8\%$ and $\eta = 2.6\%$, $\alpha = 14.6\%$ and $\eta = 2.9\%$ and $\alpha = 17.2\%$ and $\eta = = 3.4\%$ BD (f_T = 23.5 kHz, W = 100 W, d_g = 4.5 mm, $G_g = 0.83$ cm^3/s) are larger than the respective device characteristics $\alpha = 4.7\%$ and $\eta = 1.9\%$ in the absence of granules in the discharge volume (f_T = 23.5 kHz, W = 100 W, d_g = 4.5 mm) at the same volumetric gas flow rate G_g = 0.83 cm^3/s. At $G_g = 3.3$ cm^3/s, $\eta = 2.6\%$ and $\eta = 2.9\%$ determined for barium titanate $BaTiO_3$ granules with diameters of 1.25–1.4 and 1.6–1.8 mm, are less than the corresponding $\eta = 3.2\%$, obtained without granules in the discharge region with a comparable gas residence time ($\tau_T \approx 5.52$ s, f_T = 23.5 kHz, W = 100 W, d_g = 4.5 mm). At the increase in the diameter of the granules of 2.0–2.24 mm, $\eta = 3.4\%$ became larger than the corresponding $\eta = 3.2\%$ without filling the reactor with granules. The degree of CO_2 decomposition measured in a BD without granules in the reactor is $\alpha = 9.8\%$ at $\tau_T \approx 5.52$ s, f_T = 23.5 kHz, W = 100 W, d_g = 4.5 mm and $G_g = 3.3$ cm^3/s and is always less than the corresponding value $\alpha = 13.8$–17.2% in the presence in the BD reactor (f_T = 23.5 kHz, W = 100 W, d_g = 4.5 mm, $G_g = 0.83$ cm^3/s) of barium titanate $BaTiO_3$ granules with diameters of 1.25–1.4, 1.6–1.8 and 2.0–2.24 mm. Similar results were obtained for granules made of alumina Al_2O_3 with a maximum diameter of 2.0–2.24 mm. The degree of decomposition of CO_2 at filling the discharge volume with Al_2O_3 alumina granules approximately coincides with the corresponding value obtained for granules made of barium titanate $BaTiO_3$ and is $\alpha = 17\%$. The energy efficiency of the BD discharge device at f_T = 23.5 kHz, W = 100 W, d_g = 4.5 mm, $G_g = 0.83$ cm^3/s, determined in the presence of Al_2O_3 granules, is $\eta = 3.4\%$ and always higher than the corresponding values $\eta = 1.9$ and 3.2%, determined without granules in the reactor for BD conditions at f_T = 23.5 kHz, W = 100 W, d_g = 4.5 mm, $G_g = 0.83$ cm^3/s and f_T = 23.5 kHz, W = 100 W, d_g = 4.5 mm and $G_g = 3.3$ cm^3/s, respectively.

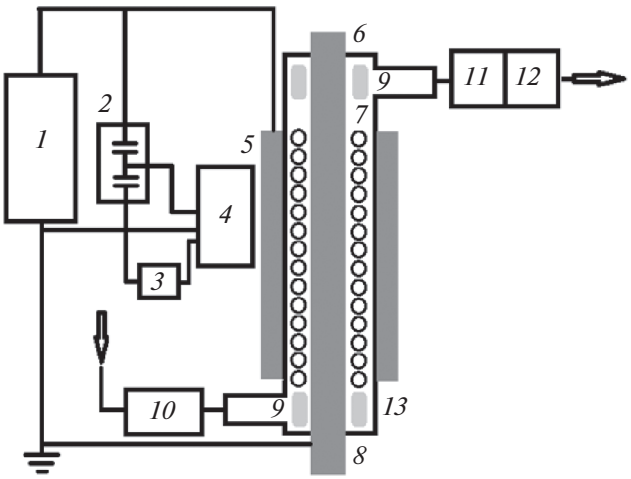

Fig. 2. *1*—barrier discharge power supply (f_T = 23.5 kHz); *2*—measuring capacities; *3*—measuring resistance; *4*—oscilloscope; *5*—outer high-voltage electrode; *6*—inner (ground) electrode (diameter of 8, 10, 12 or 13 mm); *7*—granules; *8*—inner (ground) electrode; *9*—quartz wool (or glass wool); *10* and *11*—gas-vacuum system for supplying and pumping gas, respectively; *12*—gas chromatograph; *13*—discharge tube.

Thus, the addition of spherical granules of barium titanate $BaTiO_3$ and alumina Al_2O_3 with a maximum

diameter of 2.0–2.24 mm improves the performance of the BD.

When spherical granules made of quartz SiO_2 and zirconium dioxide ZrO_2 with diameters of 1.25–1.4, 1.6–1.8 and 2.0–2.24 mm, as well as Al_2O_3 alumina granules with diameters of 1.25–1.4 mm and 1.6–1.8 mm are added into in the BD discharge volume (f_T = 23.5 kHz, W = 100 W, d_g = 4.5 mm, G_g = 0.83 cm^3/s), the α and η values decrease compared to the corresponding values α = 13.8–17.2% and η = 2.6–3.4%, α = 17% and η = 3.4% and α = 9.8% and η = 1.9%, obtained for granules of barium titanate $BaTiO_3$ with diameters of 1.25–1.4, 1.6–1.8 and 2.0–2.24 mm and alumina Al_2O_3 with a diameter of 2.0–2.24 mm and in the absence of granules in the BD discharge volume at f_T = 23.5 kHz, W = 100 W, d_g = 4.5 mm, G_g = 0.83 cm^3/s. When granules of quartz SiO_2, zirconium dioxide ZrO_2 and alumina Al_2O_3 with a diameter of 1.25–1.4 mm are added to the discharge volume, the degree of CO_2 decomposition (α = 5.5, 5.6 and 7.6%, respectively) in BD at f_T = 23.5 kHz, W = 100 W, d_g = 4.5 mm, G_g = 0.83 cm^3/s exceeds the corresponding value (α = 4.7%) measured without granules in the discharge volume of the BD at f_T = 23.5 kHz, W = 100 W, d_g = 4.5 mm, G_g = 3.3 cm^3/s and the same gas residence time $\tau_T \approx$ 5.52 s in the reactor. On the contrary, the BD energy efficiency (η = 1, 1.2, and 1.4%) at f_T = 23.5 kHz, W = 100 W, d_g = 4.5 mm, G_g = 0.83 cm^3/s and the addition of granules from quartz SiO_2, zirconium dioxide ZrO_2 and alumina Al_2O_3 into the discharge volume is less than η = 3.2% for BD without granules at $\tau_T \approx$ 5.52 s, f_T = 23.5 kHz, W = 100 W, d_g = 4.5 mm, G_g = 3.3 cm^3/s. At the increase in the diameter (1.6–1.8 mm to 2.0–2.24 mm) of silica SiO_2 granules, the measured values α = 3.3 and 4.7%, and η = 0.6 and 0, 8% become less than the values α = 4.7% and η = 3.2% in the absence of granules in the BD and $\tau_T \approx$ 5.52 s, f_T = 23.5 kHz, W_A = 100 W, d_g = 4, 5 mm, G_g = 3.3 cm^3/s. For granules of zirconium dioxide ZrO_2 and alumina Al_2O_3 with diameters of 1.6–1.8 mm, the measured values of the degree of decomposition of carbon dioxide α = 4.9 and 8.5%, respectively, exceed the value α = 4.7%, measured in the absence of granules in the discharge volume. The energy efficiency of the device η = 0.9 and 1.7% for granules of zirconium dioxide ZrO_2 and alumina Al_2O_3, respectively, is always less than the value η = 3.2% in the absence of granules in the BD reactor and $\tau_T \approx$ 5.52 s, f_T = 23.5 kHz, W = 100 W, d_g = 4.5 mm, G_g = 3.3 cm^3/s. When zirconium dioxide ZrO_2 granules with a maximum diameter of 2.0–2.24 mm are added to the BD reactor at f_T = 23.5 kHz, W_A = 100 W, d_g = 4.5 mm, G_g = 0.83 cm^3/s, the operating device parameters α and η take values of 7.5% and 1.4%, respectively. The degree of decomposition CO_2 is larger than α = 4.7%, and the energy efficiency is less than η = 3.2% in the absence of granules in the discharge volume.

Thus, the maximum values of the degree of decomposition of carbon dioxide $\alpha_M \approx$ 17% and the energy efficiency of the device $\eta_M \approx$ 3.4% are obtained by adding granules of barium titanate $BaTiO_3$ and alumina Al_2O_3 with a diameter of 2.0–2.24 mm to the BD reactor at f_T = 23.5 kHz, W = 100 W, d_g = 4.5 mm, G_g = 0.83 cm^3/s.

In [48], it was found that the active power W_A depends weakly on the material of the granules: for SiO_2 granules, 61 ± 1 W; for ZrO_2 granules, 57 ± 5 W; for Al_2O_3 granules, 60 ± 4 W; for $BaTiO_3$ granules, 61 ± 3 W. The breakdown voltage of the discharge volume V_b filled with granules depends on their permittivity ε_g of granules, as found in [93]: V_b = 1.47 kV for quartz SiO_2 (ε_g = 3.9); V_b = 0.82 kV for zirconium dioxide ZrO_2 (ε_g = 25); V_b = 1.84 kV for alumina Al_2O_3 (ε_g = 9.1); V_b = 0.97 kV for barium titanate $BaTiO_3$ (ε_g = 4000).

It was established in [48] that the minimum α and η values are obtained when the reactor is filled with SiO_2 quartz granules. When granules of zirconium dioxide ZrO_2, alumina Al_2O_3 and barium titanate $BaTiO_3$are added to the reactor, there is an increase in the values of the operational characteristics of the discharge device α and η in the indicated sequence. The dependence of the parameters α and η on the size and physico-chemical characteristics of the material of the granules is not linear. It was shown in [33] that the spatial distribution of BD parameters is determined by the arrangement of contacts between different granules and between granules and the surface of the reactor wall. The applied potential difference between the electrodes of the BD reactor causes the polarization of the granules and increases the electric field strength near the contact points, which leads to an increase in the average electron energy [94]. The α values increase with increasing dielectric constant ε_g from 3.9 (for quartz SiO_2) to 4000 (for barium titanate $BaTiO_3$). The results of the measurements of α for zirconium dioxide ZrO_2 and alumina Al_2O_3 materials do not confirm this dependence. The established dependences of α on the granule diameter d_g for the materials of alumina Al_2O_3, barium titanate $BaTiO_3$ and quartz SiO_2, zirconium dioxide ZrO_2 also differ. In [93], a BD model in helium was developed when the reactor is filled with granules with a given permittivity. It is shown that the spatial distribution of the electron density and average energy in the discharge gap, the conduction current, and the electric field strength depend on the dielectric granule permeability ε_g, but not on their size.

In [48], the highest α and η values were obtained using the largest spherical granules (2.0–2.24 mm) of

barium titanate $BaTiO_3$ (see Table 1). In accordance with simulation results obtained in [93], the electric field strength increases with increasing dielectric permeability, but does not increase with an increase in the size of $BaTiO_3$ granules. Calculations show that a simultaneous increase in the dielectric constant and the diameter of spherical granules leads to an increase in the electric field and electron density. As a result, the performance of the discharge device is improved. It was found in [93, 95] that an increase in the surface roughness of the granules leads to an increase in the α and η values. The nonlinear character of the dependence of α and η values on the surface roughness of the granules indicates that the α and η values are also determined by the acidity and surface area, specific and molar heat capacity, total volume and size of open pores of the granules.

The electric field strength is also determined by the porosity and pore size of the granules [48]. The porosity of spherical Al_2O_3 alumina granules is produced during their sintering at 1540°C. It was found in [48] that granules made of quartz SiO_2 and zirconium dioxide ZrO_2 have very low porosity, while both Al_2O_3 alumina and $BaTiO_3$ barium titanate granules have higher porosity. The average pore size for Al_2O_3 alumina granules is 0.08 μm. It is an order of magnitude smaller than the average pore size of 0.87 μm for barium titanate $BaTiO_3$ granules. It was shown in [96] that gas discharge plasma is not formed in pores with a size of 0.87 μm. It is not ruled out in [97] that streamers can penetrate inside the pore. The field strength increases at the edges of the pores of the granule.

Thus, when granules are added to the reactor, the α and η values depend on their porosity. The increase in α and η values is especially pronounced for Al_2O_3 alumina granules and barium titanate $BaTiO_3$.

It was found in [48] that for granules made of quartz SiO_2, the α and η values change nonmonotonically depending on their size and in the following order: 1.6–1.8 mm < 2.0–2.24 mm < 1.25–1.4 mm. For granules made from zirconium dioxide ZrO_2, a nonmonotonic dependence of the α and η values on their size is also observed. The α and η values increase in the following order of the change in their diameter: 1.6–1.8 mm < 1.25–1.4 mm < 2.24 mm. For granules made of alumina Al_2O_3 and barium titanate $BaTiO_3$, the α and η values increase monotonically with the increase of the granule size as 1.25–1.4 mm < 1.6–1.8 mm < 2.24 mm. The explanation for the observed dependence of α and η on the material and size of the granules added to the reactor is as follows. The increase in the values of α and η is due to the change in the spatial distribution of the electric field strength in the reactor as a result of the induced polarization and accumulation of charges on the surface of dielectric spherical granules. The spatial distribution of the electric field strength depends on the contact angle between the granules and between the granules and the surface of the reactor tube, on the number of contact points, and on the curvature and permittivity of the granules [33, 93, 98]. It was shown in [33, 98] that the number of contact points increases with decreasing granule size.

Thus, an increase in the permittivity of granules [93] and a decrease in their size [33, 98] leads to an increase in the of α and η values.

According to the results of [48], the amount of accumulated charge on the surface of dielectric spherical granules decreases with an increase in the size of the granules and the volume of the reactor free from granules. The free electron density involved in the CO_2 decomposition reaction increases with increasing granule size. As a result, the α and η values increase. In [48], the results of determining the α and η values for a constant ratio between the average granule size and the size of the discharge gap, but with varying sizes, and for a constant granule size but the gap size varied, are given; for a constant gap size but varying granule size. It was found that in a BD at f_T = 23.5 kHz, $G_g = 0.83$ cm^3/s and $W = 100$ W, the α and η values increase from 18 to 26% and from 3 to 4%, respectively, when the active power W_A in the range of ≈67–68 W and an increase in the size of the discharge gap from 2 mm to 3.5 mm and barium titanate $BaTiO_3$ granules (1.18–1.25, 1.4–1.6 and 2.0–2.24 mm) at a constant ratio between them (≈0.6). When the ratio of the granule size to the gap size decreases from 0.6 to 0.5, the α and η values decrease from 26 to 20% and from 4 to 3.3%, respectively. The size of the granules remained constant and lay in the range of 2–2.24 mm, while the size of the discharge gap increased from 3.5 to 4.5 mm. As a result, data for α and η were obtained with a larger number of granules in the discharge volume. At the increase in the ratio of the granule size to the gap size from 0.3 to 0.5, the α and η values increase from 16 to 20% and from 2.6 to 3.3%, respectively. The size of the discharge gap remained constant at 4.5 mm, while the size of the granules increased from 1.25–1.4 to 2–2.24 mm. The maximum values $\alpha_M = 20\%$ and $\eta_M = 3.3\%$ at $d_g = 4.5$ mm are less than the corresponding values $\alpha_M = 26\%$ and $\eta_M = 4\%$ at $d_g = 3.5$ mm. A noticeable change in α and η with increasing granule size at the constant ratio of the granule size to the gap size is due to the remaining number of granules in the reactor and, consequently, the number of contact points between granules and between granules and the wall of the reactor tube. In the case of the constant gap size, the number of contact points decreases as the grain size increases.

Thus, the best operational parameters of a discharge device based on a barrier discharge when granules of barium titanate $BaTiO_3$ are added to the reactor are obtained taking into account the optimization of the ratio between the granule sizes and the discharge gap [48]. This conclusion is confirmed by the results of

Table 1. Designs and parameters of discharge devices based on barrier discharge for CO_2 decomposition

Characteristics of the discharge device	Range of gas discharge parameters	@Ссылка 1
A pair of coaxial quartz tubes, with conductive linings on the outer and inner surfaces, gas – CO_2	p = 500 Torr, W = 0.1 kW, G_g = 22 cm^3/s, E_V^J = 18–800 J/cm^3, α = 3–300%, η = 0.4–1%, T_g = 415–515 K, T_e = 1–3 eV	[9, 14]
Coaxial outer quartz tub (R_1 = 1 cm, d_ε = 2 mm) with a conductive lining on the outer surface and an inner steel rod (R_e = 0.6 cm), f_T =10–30 kHz, L = 280 mm, d_g = 2 mm, gas – CO_2	p = 760 Torr, W_A = 0.056–0.143 kW, G_g = 3.3 cm^3/s, V_b = 4.4–4.8 kV, V_d = 3.6–4.0 kV, α = 5–13%, η = 3.3–3.7%, V_A = 5.6–7.3 kV	[55]
Coaxial outer quartz tube (R_1 = 1.25 cm, d_ε =1.5, 2, 2.2 mm) with a conductive lining on the outer surface and an inner steel rod (R_e = 0.75–0.85 cm), f_T = 8, 9, 10, 11 kHz, L = 60, 100, 140 mm, d_g = 2.5, 3.0, 3.5 mm, gas – CO_2	p = 760 Torr, W_A = 0.01–0.05 kW, G_g = 0.42–2.2 cm^3/s, α = 12.6–27.2%, η = 2.3–9%, $V_A \le$ 30 kV	[51]
A pair of coaxial quartz tubes, with conductive plates on the outer (R_1 = 1.75 cm, d_ε = 1.5) and inner (R_2 = 1 cm, d_ε = 1.5 mm) surfaces, f_T = 25 kHz, L = 173, d_g = 7.5 mm, gas – mixture (100%-X)CO_2 + XCO_2, 0 ≤ X ≤ 50%, granules ($BaTiO_3$), d_ε = 3 mm	p = 760 Torr, W_A = 0.046–0.1 kW, G_g = 0.42–1.7 cm^3/s, τ_T = 2.1–4.2 s, α = 16%, η = 2%, $V_A \le$ 20 kV, $T_W \approx T_g \approx$ 373 K	[59]
Coaxial outer (quartz/ceramic Al_2O_3) tube (R_1 = 0.85 cm, d_ε = 0 mm) with a conductive lining on the outer surface and an inner steel rod (R_e = 0.4, 0.5, 0.6, 0.65 cm), f_T = 23,5 kHz, L = 100 mm, d_g =2, 2.5, 3.5, 4 mm, gas – CO_2, glass wool, quartz wool granules (SiO_2), d_ε = 1.18–1.25, 1.25–1.4, 1.6–1.8, 2.0–2.24 mm granules (ZrO_2), d_ε = 1.18–1.25, 1.25–1.4, 1.6–1.8, 2.0–2.24 mm, granules (Al_2O_3), d_ε = 1.25–1.4, 1.6–1.8, 2.0–2.24 mm, granules ($BaTiO_3$), d_ε = 1.25–1.4, 1.6–1.8, 2.0–2.24 mm	p = 760 Torr, W = 0.1 kW, W_A = 0.0577–0.061 kW, G_g = 0.8, 3.3 cm^3/s, V_b = 0.8–1.8 kV, τ_T = 5.52 s, α = 25%, η = 4.5%, $T_W \approx T_g \approx$ 419 K	[48]

The first and second columns list the main design elements of the device and the BD parameters: p is the static gas pressure in the reactor (Torr); f_T is the frequency of the applied high voltage to the electrodes (kHz); V_A is the high voltage amplitude (kV); V_b is the minimum value of the breakdown voltage of the discharge gap (kV); V_d is the maximum value of the voltage across the discharge gap during the BD (kV); G_g is the volumetric flow rate of gas (cm^3/s); L and d_g are the longitudinal and transverse dimensions of the discharge volume, respectively (mm); W is the power of the power source supplied to the reactor (kW); T_W is the temperature of the reactor wall (K); d_g is the diameter of spherical granules added to the reactor of the discharge device (mm); τ_T is the residence duration of particles in the discharge volume (s); R_1 and R_2 are the outer radius of the outer and inner radius of the inner, respectively, of the reactor tubes (cm); dη is the tube wall thickness (mm); R_e is the outer radius of the inner electrode (cm). They are supplemented by the results of determining the values of the operational characteristics of the discharge device (α and η) and the parameters of the BD plasma: T_g is the translational gas temperature (K); α is the degree of CO2 decomposition (%); η is the energy efficiency of the discharge device (%); T_e is the electron temperature in the BD (eV); E_V^J is the specific energy absorbed by the barrier discharge plasma per unit volume (J/cm^3); W_A is the active power absorbed by the barrier discharge plasma (kW).

[33], in which the dependence of the operational characteristics of the device on the size of the discharge gap and granules of zirconium dioxide ZrO_2 added to the reactor was studied. For ZrO_2 zirconia granules, the best performance is obtained with a granule- size-to-gap-size ratio of 0.3. It is important to emphasize that in order to achieve the maximum operational characteristics of the device α and η, it is necessary to addi-

tionally take into account many parameters: the size of the discharge gap; voids between granules (their number and size); the number of points of contact between the granules and between the granules and the reactor tube.

Research [32, 48] is devoted to studying the dependence of the operational characteristics of the device on the presence or absence of glass/quartz wool added into the reactor. In [32], a BD was used in the studies at a gas volume flow $G_g = 0.3$ cm^3/s, a frequency $f_T =$ 18 kHz, and a discharge gap $d_g = 0.6$ mm. Aluminum foil was used as an outer electrode. It was established that in the absence of quartz wool in reactor $\alpha =$ 14.6%, and when it is added to the reactor $\alpha = 24.4\%$. In [48], the performance characteristics were determined in the absence of glass wool or quartz wool in the reactor, when glass wool was placed at the reactor inlet and outlet outside the discharge volume, and also in a reactor completely filled with glass wool. The power W supplied to the reactor at a frequency of 23.5 kHz was 100 W with a discharge gap of 4.5 mm. The active power W_A absorbed by the barrier discharge plasma was 67 ± 2 W. The experiments were carried out at two different volumetric gas flow rates $G_g = 0.83$ and 3.3 cm^3/s. It has been established that the α and η values, determined in the presence and absence of glass wool in the reactor, coincide within the limits of the determination error. The degrees of CO_2 decomposition measured at $G_g = 0.83$ and 3.3 cm^3/s are 10–11 and 5–6%, respectively. The energy efficiency of the discharge device lies in the ranges of 1.7–1.9% and 3–4% at the same gas flow rates. The results of [48] are explained by the authors by the fact that the dependence of the operational characteristics of the discharge device on the residence time of gas in the discharge volume plays a more important role than their dependence on the electric field strength in the reactor when glass wool (made of SiO_2 quartz material), which is characterized by a low dielectric constant, is placed in the reactor. The difference between the results obtained in [32] and [48] is explained by the difference of BD parameters and designs of discharge devices. The main difference between the designs of discharge devices is the size of the discharge gaps of 4.5 mm [48] and 0.6 mm [32]. To explain the difference between the results of [48] and [32], CO_2 decomposition was studied in [48] at different sizes of the discharge gap d_g: 268, 455, 705, and 1230 μm. It is found that with decreasing gap size d_g, the degree of decomposition of carbon dioxide α increases in an empty reactor from 11 to 54%, and when glass wool (or quartz wool) is added to the reactor, from 1% to 47%. This is explained by an increase in the electric field and an increase in the average electron energy with a decrease in the discharge gap [94]. To ensure the same residence time in the discharge volume of the gas, of approximately 7.5 s, in the absence and presence of glass wool in the reactor (in the range of the discharge gap of 268–1230 μm), the experiments in [48] were performed at different gas volume flow rates. It is shown that the values of $\alpha = 54$ and 51%, measured without glass wool/quartz wool in the reactor at discharge gap sizes of $d_g = 268$ and 455 μm, respectively, are larger than those when the reactor is filled with glass wool $\alpha = 49$ and 48%. With an increase in the size of the discharge gap ($d_g = 705$ and 1230 μm), the values of $\alpha = 35.6$ and 30%, measured in the absence of glass wool in the reactor, are less than when the reactor is filled with glass wool $\alpha = 46.7$ and 48.8%. This is in agreement with the results of [32]. In [48], for comparison with the data from [32], the results of measurements of α and η in a BD ($W = 100$ W, $G_g =$ 0.83 cm^3/s, $f_T = 23.5$ kHz, inner stainless steel electrode, $d_g = 4.5$ mm) from the material of the dielectric tube of the reactor and the material of the wool added to the reactor are presented. The outer electrode, as in [32], was made of aluminum foil. The α and η values measured in the case of filling a glass tube with glass and quartz wool differ slightly and are $\alpha = 10.5\%$ and $\eta = 1.7\%$ and $\alpha = 9.8\%$ and $\eta = 1.4\%$, respectively. They are smaller than the corresponding values $\alpha \approx$ 11% and $\eta \approx 1.9\%$ in the absence of quartz/glass wool in the reactor. When replacing a glass tube with a quartz one, the α and η values obtained in the case of filling the reactor with glass and quartz wool are $\alpha =$ 7.2%, $\eta = 1.4\%$ and $\alpha = 9.8\%$, $\eta = 1.1\%$, respectively. They are smaller than the corresponding values ($\alpha \approx$ 11% and $\eta \approx 1.9\%$) obtained for the case of an empty reactor.

Thus, it was shown in [48] that the α and η values depend insignificantly on the material of wool added into the reactor. The results obtained in [48] are consistent with the corresponding results of studies of CH_4 reforming with CO_2 [99].

In [48], the dependence of the α and η values on the dielectric material of the reactor tube (quartz SiO_2/alumina Al_2O_3) and the material of spherical granules (1.6–1.8 mm in diameter, quartz SiO_2/alumina Al_2O_3) added into the BD reactor ($W = 100$ W, $G_g = 0.83$ cm^3/s, $f_T = 23.5$ kHz, stainless steel inner electrode, $d_g = 4.5$ mm). It was established that α and η measured in reactors made of quartz (SiO_2) and alumina (Al_2O_3) containing quartz (SiO_2) granules differ little and are $\alpha = 2.9\%$, $\eta = 0.4\%$ and $\alpha = 3.8\%$, $\eta =$ 0.6%, respectively. This conclusion is also valid in the case of filling the reactor with Al_2O_3 alumina granules. The α and η values for the reactor made of quartz are $\alpha = 10.6\%$ and $\eta = 2.6\%$, respectively, and coincide within the error with the corresponding values $\alpha =$ 9.7% and $\eta = 1.7\%$, measured in a reactor made of alumina Al_2O_3.

To further improve the performance of a BD-based discharge device for CO_2 decomposition, it is required: to search for an optimal catalyst applied to granules; to increase the number of contact points

between the granules and between the granules and the surface of the reactor tube while maintaining the maximum void volume and the ratio of the granule size and the discharge gap. The presented results show that the method of plasma catalysis of CO_2 decomposition is potentially interesting.

CONCLUSIONS

Thus, the maximum values of the degree of decomposition of CO_2 α and the energy efficiency of the discharge device η, obtained in experiments with BD, do not exceed $\alpha \le 70\%$ and $\eta \le 23\%$. Note that the maximum parameter values are not achieved at the same time. Experimental and theoretical studies of the mechanism of carbon dioxide decomposition show that the decomposition of a molecule differs from thermal decomposition: the decomposition of carbon dioxide CO_2 occurs under nonequilibrium conditions as a result of dissociative excitation of a carbon dioxide molecule by electron impact. The contribution of reactions involving vibrationally excited CO_2 molecules to the decomposition rate of CO_2 can be neglected. To improve the characteristics of a BD-based discharge device, it is necessary to improve designs of the discharge device: to keep the temperature of the reactor wall as low as possible, to provide high values of the residence time of the gas in the discharge volume and the charge due to the conduction current, etc.

At present, a promising direction for increasing α and η in BD, the same as in other types of discharge is the use of plasma-catalytic systems. At the same time, it should be noted that in many cases the BD volume is filled with granules of materials that are not catalysts in the conventional sense. The change in the efficiency of BD-based devices in this case is achieved by changing their electrodynamic characteristics and is not associated with catalysis as such. We note that also in the case of using fillers with a catalyst (as a rule, metals) also changes the electrodynamic characteristics of the discharge device, and it is difficult to separate this effect from a purely catalytic effect in decomposition of carbon dioxide. This problem requires further research.

FUNDING

The work was supported by the State task of the A.V. Topchiev Institute of Petrochemical Synthesis, Russian Academy of Sciences, Moscow.

CONFLICT OF INTEREST

The authors declare that they have no conflicts of interest.

REFERENCES

1. B. M. Smirnov, Sov. Phys.-Usp. **21**, 978 (1978).
2. C. S. Song, Catal. Today **115**, 2 (2006).
3. G. Centi and S. Perathoner, Catal. Today **148**, 191 (2009).
4. I. Omae, Coord. Chem. Rev. **256**, 1384 (2012).
5. I. Dimitriou, P. Garcia-Gutierrez, R. H. Elder, R. M. Cuéllar-Franca, A. Azapagic, and R. W. K. Allen, Energy Environ. Sci. **8**, 1775 (2015).
6. E. V. Kondratenko, G. Mul, J. Baltrusaitis, G. O. Larrazábal, and J. Pérez-Ramirez, Energy Environ. Sci. **6**, 3112 (2013).
7. M. Mikkelsen, M. Jørgensen, and F. C. Krebs, Energy Environ. Sci. **3**, 43 (2010).
8. P. Lahijani, Z. A. Zainal, M. Mohammadi, and A. R. Mohamed, Renewable Sustainable Energy Rev. **41**, 615 (2015).
9. V. D. Rusanov and A. A. Fridman, *Physics of Chemically Active Plasma.* (Nauka, Moscow, 1984) [in Russian].
10. A. Fridman, *Plasma Chemistry.* (Cambridge University Press, New York, 2008).
11. R. Snoeckx and A. Bogaerts, Chem. Soc. Rev. **46**, 5805 (2017).
12. A. George, B. Shen, M. Craven, Y. Wang, D. Kang, C. Wu, and X. Tu, Renewable Sustainable Energy Rev. **135**, 109702 (2021).
13. Yu. A. Lebedev and V. A. Shakhatov, Russ. J. Appl. Chem. **95**, 1 (2022).
14. Yu. P. Andreev, Zh. Fiz. Khim. **38**, 794 (1964).
15. J. Wang, G. Xia, A. Huang, S. L. Suib, Y. Hayashi, and H. Matsumoto, J. Catal. **185**, 152 (1999).
16. R. Li, Y. Yamaguchi, S. Yin, Q. Tang, and T. Sato, Solid State Ionics **172**, 235 (2004).
17. R. Li, Q. Tang, S. Yin, and T. Sato, Fuel Process. Technol. **87**, 617 (2006).
18. R. Li, Q. Tang, S. Yin, and T. Sato, Appl. Phys. Lett. **90**, 131502 (2007).
19. R. J. Leiweke and B. N. Ganguly, Appl. Phys. Lett. **90**, 241501 (2007).
20. S. Paulussen, B. Verheyde, X. Tu, C. De Bie, T. Martens, D. Petrovic, A. Bogaerts, and B. Sels, Plasma Sources Sci. Technol. **19**, 034015 (2010).
21. Y. Tagawa, S. Mori, M. Suzuki, I. Yamanaka, T. Obara, J. Ryu, and Y. Kato, Kagaku Kogaku Ronbunshu **37**, 114 (2011).
22. Q. Yu, M. Kong, T. Liu, J. Fei, and X. Zheng, Plasma Chem. Plasma Process. **32**, 153 (2012).
23. S. Wang, Y. Zhang, X. Liu, and X. Wang, Plasma Chem. Plasma Process. **32**, 979 (2012).
24. R. Aerts, T. Martens, and A. Bogaerts, J. Phys. Chem. C **116**, 23257 (2012).
25. A. Michelmore, D. A. Steele, J. D. Whittle, J. W. Bradley, and R. D. Short, RSC Adv. **3**, 13540 (2013).
26. F. Brehmer, S. Welzel, M. C. M. van de Sanden, and R. Engeln, J. Appl. Phys. **116**, 123303 (2014).
27. M. A. Lindon and E. E. Scime, Front. Phys. **2**, 1 (2014). https://www.frontiersin.org/article/10.3389/fphy.2014.00055.
28. D. Mei, X. Zhu, Y.-L. He, J. D. Yan, and X. Tu, Plasma Sources Sci. Technol. **24**, 015011 (2015).
29. T. Kozák and A. Bogaerts, Plasma Sources Sci. Technol. **23**, 045004 (2014).

30. R. Aerts, W. Somers, A. Bogaerts, ChemSusChem **8**. 702 (2015).
31. M. Ramakers, I. Michielsen, R. Aerts, V. Meynen, and A. Bogaerts, Plasma Processes Polym. **12**, 755 (2015).
32. X. Duan, Z. Hu, Y. Li, and B. Wang, AIChE J. **61**, 898 (2015).
33. K. Van Laer and A. Bogaerts, Energy Technol. **3**, 1038 (2015).
34. X. Duan, Y. Li, W. Ge, and B. Wang, Greenhouse Gases: Sci. Technol. **5**, 131 (2015).
35. R. Snoeckx, Y. X. Zeng, X. Tu, and A. Bogaerts, RSC Adv. **5**, 29799 (2015).
36. D. H. Mei, X. B. Zhu, Y. L. He, J. D. Yan, and X. Tu, Plasma Sources Sci. Technol. **24**, 015011 (2015).
37. R. Snoeckx, S. Heijkers, K. V. Wesenbeeck, S. Lenaerts, and A. Bogaerts, Energy Environ. Sci. **9**, 999 (2016).
38. M. Schiorlin, R. Klink, and R. Brandenburg, Eur. Phys. J.: Appl. Phys. **75**, 24704 (2016).
39. I. Belov, S. Paulussen, and A. Bogaerts, Plasma Sources Sci. Technol. **25**, 15023 (2016).
40. T. Butterworth, R. Elder, and R. Allen, Chem. Eng. J. **293**, 55 (2016).
41. S. Ponduri, M. M. Becker, S. Welzel, M. C. M. van de Sanden, D. Loffhagen, and R. Engeln, J. Appl. Phys. **119**, 093301 (2016).
42. A. Bogaerts, C. De Bie, R. Snoeckx, and T. Kozák, Plasma Processes Polym. **14**, 1600070 (2016).
43. M. Grofulović, L. L. Alves, and V. Guerra, J. Phys. D: Appl. Phys. **49**, 395207 (2016).
44. A. Bogaerts, W. Wang, A. Berthelot, and V. Guerra, Plasma Sources Sci. Technol. **25**, 55016 (2016).
45. D. Mei, X. Zhu, C. Wu, B. Ashford, P. T. Williams, and X. Tu, Appl. Catal., B **182**, 525 (2016).
46. A. Ozkan, T. Dufour, T. Silva, N. Britun, R. Snyders, A. Bogaerts, and F. Reniers, Plasma Sources Sci. Technol. **25**, 025013 (2016).
47. A. Ozkan, A. Bogaerts, and F. Reniers, J. Phys. D: Appl. Phys. **50**, 084004 (2017).
48. I. Michielsen, Y. Uytdenhouwen, J. Pype, B. Michielsen, J. Mertens, F. Reniers, V. Meynen, and A. Bogaerts, Chem. Eng. J. **326**, 477 (2017).
49. A. Bogaerts, A. Berthelot, S. Heijkers, St. Kolev, R. Snoeckx, S. Sun, G. Trenchev, K. Van Laer, and W. Wang, Plasma Sources Sci. Technol. **26**, 063001 (2017).
50. P. Koelman, S. Heijkers, S. T. Mousavi, W. Graef, D. Mihailova, T. Kozak, A. Bogaerts, and J. van Dijk, Plasma Processes Polym. **14**, 1600155 (2017).
51. D. Mei and X. Tu, J. CO2 Util. **19**, 68 (2017).
52. D. Mei and X. Tu, ChemPhysChem. **18**, 3253 (2017).
53. K. Zhang, G. R. Zhang, X. T. Liu, A. N. Phan, and K. Luo, Ind. Eng. Chem. Res. **56**, 3204 (2017).
54. S. Xu, J. C. Whitehead, and P. A. Martin, Chem. Eng. J. **327**, 764 (2017).
55. P. Chen, J. Shen, T. Ran, T. Yang, and Y. Yin, Plasma Sci. Technol. **19**, 125505 (2017).
56. N. Lu, D. Sun, C. Zhang, N. Jiang, K. Shang, X. Bao, J. Li, and Y. Wu, J. Phys. D: Appl. Phys. **51**, 094001 (2018).
57. S. J. Xu, P. I. Khalaf, P. A. Martin, and J. C. Whitehead, Plasma Sources Sci. Technol. **27**, 075009 (2018).
58. B. Ashford, Y. Wang, C.-K. Poh, L. Chen, and X. Tu, Appl. Catal., B **276**, 119110 (2020).
59. K. Zhang and A. P. Harvey, Chem. Eng. J. **405**, 126625 (2021).
60. V. T. Samoilovich, V. I. Gibalov, and K. V. Kozlov, *Physical Chemistry of Barrier Discharge* (Izd. Mosk. Gos. Univ., Moscow, 1989) [in Russian].
61. B. Eliasson and U. Kogelschatz, IEEE Trans. Plasma Sci. **19**, 309 (1991).
62. B. Eliasson, W. Egli, and U. Kogelschatz, Pure Appl. Chem. **66**, 1275 (1994).
63. U. Kogelschatz, Plasma Chem. Plasma Process. **23**, 1 (2003).
64. J. J. Lowke, A. V. Phelps, and B. W. Irwin, J. Appl. Phys. **44**, 4664 (1973).
65. T. G. Beuthe and J. S. Chang, Jpn. J. Appl. Phys. **36**, 4997 (1997).
66. Yu. A. Lebedev and V. A. Shakhatov, High Energy Chem. **55**, 419 (2021).
67. Yu. A. Lebedev and V. A. Shakhatov, Usp. Prikl. Fiz. **9**, 365 (2021).
68. H. L. Chen, H. M. Lee, S. H. Chen, and M. B. Chang, Ind. Eng. Chem. Res. **47**, 2122 (2008).
69. G. J. M. Haelaar and L. C. Pitchford, Plasma Sources Sci. Technol. **14**, 722 (2005).
70. X. Tu, H. J. Gallon, M. V. Twigg, P. A. Gorry, and J. C. Whitehead, J. Phys. D: Appl. Phys. **44**, 274007 (2011).
71. S. Y. Liu, D. H. Mei, Z. Shen, and X. Tu, J. Phys. Chem. C **118**, 10686 (2014).
72. A. Meiners, M. Leck, and B. Abel, Rev. Sci. Instrum. **81**, 113507 (2010).
73. B. Wang, W. Yan, W. Ge, and X. Duan, J. Energy Chem. **22**, 876 (2013).
74. A. Indarto, D. R. Yang, J. W. Choi, H. Lee, and H. K. Song, J. Hazard. Mater. **146**, 309 (2007).
75. A. Ozkan, T. Dufour, A. Bogaerts, and F. Reniers, Plasma Sources Sci. Technol. **25**, 045016 (2016).
76. D. Mei, Y.-L. He, S. Liu, J. Yan, and X. Tu, Plasma Processes Polym. **13**, 544 (2016).
77. W. Xu, M.-W. Li, G.-H. Xu, and Y.-L. Tian, Jpn. J. Appl. Phys. **43**, 8310 (2004).
78. S.-Z, Li, J.-P. Lim, J. G. Kang, and H. S. Uhm, Phys. Plasmas **13**, 093503 (2006).
79. X. Tu, H. J. Gallon, and J. C. Whitehead, IEEE Trans. Plasma Sci. **39**, 2900 (2011). https://doi.org/10.1109/TPS.2011.2150247
80. M. S. Moss, K. Yanallah, R. W. K. Allen, and F. Pontiga, Plasma Sources Sci. Technol. **26**, 035009 (2017).
81. T. Takuma, IEEE Trans. Electr. Insul. **26**, 500 (1991).
82. E. C. Neyts, K. Ostrikov, M. K. Sunkara, and A. Bogaerts, Chem. Rev. **115**, 13408 (2015).
83. J. Van Durme, J. Dewulf, C. Leys, and H. Van Langenhove, Appl. Catal., B **78**, 324 (2008).
84. H. L. Chen, H. M. Lee, S. H. Chen, M. B. Chang, S. J. Yu, and S. N. Li, Environ. Sci. Technol. **43**, 2216 (2009).

85. H. L. Chen, H. M. Lee, S. H. Chen, Y. Chao, and M. B. Chang, Appl. Catal., B **85**, 1 (2008).
86. J. C. Whitehead, Pure Appl. Chem. **82**, 1329 (2010).
87. Y. Zeng, X. Zhu, D. Mei, B. Ashford, and X. Tu, Catal. Today **256**, 80 (2015).
88. H. K. Song, J.-W. Choi, S. H. Yue, H. Lee, B.-K. Na, and H. K. Songu, Catal. Today **89**, 27 (2004).
89. J. Sentek, K. Krawczyk, M. Młotek, M. Kalczewska, T. Kroker, T. Kolb, A. Schenk, K.-H. Gericke, and K. Schmidt-Szałowski, Appl. Catal., B **94**, 19 (2010).
90. X. Tu, H. J. Gallon, M. V. Twigg, P. A. Gorry, and J. C. Whitehead, J. Phys. D: Appl. Phys. **44**, 274007 (2011).
91. M. Kraus, W. Egli, K. Haffner, B. Eliasson, U. Kogelschatz, and A. Wokaun, Phys. Chem. Chem. Phys. **4**, 668 (2002).
92. A. Bogaerts, T. Kozák, K. van Laer, and R. Snoeckx, Faraday Discuss. **183**, 217 (2015).
93. K. Van Laer and A. Bogaerts, Plasma Sources Sci. Technol. **26**, 085007 (2017).
94. K. Van Laer and A. Bogaerts, Plasma Process. Polym. **14**, 1600129 (2017).
95. J. C. Whitehead, J. Phys. D. Appl. Phys. **49**, 243001 (2016).
96. Y. R. Zhang, K. Van Laer, E. C. Neyts, and A. Bogaerts, Appl. Catal., B **185**, 56 (2016).
97. Y. Zhang, H.-Y. Wang, Y.-R. Zhang, and A. Bogaerts, Plasma Sources Sci. Technol. **26**, 054002 (2017).
98. K. Van Laer and A. Bogaerts, Plasma Sources Sci. Technol. **25**, 015002 (2016).
99. H. J. Gallon, X. Tu, and J. C. Whitehead, Plasma Process. Polym. **9**, 90 (2012).

Translated by L. Mosina

SPELL: 1. Ссылка